

## STRUCTURAL AND MORPHOLOGICAL CHARACTERIZATION OF HIGHLY ALIGNED FERROMAGNETIC PVDF/Fe<sub>3</sub>O<sub>4</sub> NANOCOMPOSITE COATING

DILARA SADIGOVA<sup>1</sup>, RASIM JABBAROV<sup>2</sup>

<sup>1</sup>*Nanotechnology Laboratory, Department of Chemical Engineering, School of Science and Engineering, Khazar University, Baku Azerbaijan*

<sup>2</sup>*Institute of Physics Ministry of Science and Education of Azerbaijan.*

\**e-mail: dilara.sadigova3377@gmail.com*

\*\**e-mail: rasim.jabbarov69@gmail.com*

PVDF is a semi-crystalline fluoropolymer and has attracted a lot of interest in a variety of industrial applications because of its special qualities, which include thermal stability, chemical resistance, and piezoelectricity. A polar phase is present in the  $\beta$ -phase. Sensors, actuators, energy harvesting systems, batteries, filters, chemical warfare defense, magnetoelectric, and polymer-based composites were among the many applications it was found to have. In this work, the  $\beta$ -phase fraction of the PVDF/Fe<sub>3</sub>O<sub>4</sub> nanocomposite was measured by X-Ray diffraction analysis.

**Keywords:** PVDF; Fe<sub>3</sub>O<sub>4</sub>; X-ray diffraction;  $\beta$ -phase; nanocoating; high electroactive phase; electrospinning;

**DOI:**10.70784/azip.1.2025132

### INTRODUCTION

PVDF is a thermoplastic fluoropolymer that is extremely nonreactive and is made by polymerizing vinylidene difluoride. It can display effective ferroelectric, pyroelectric, and piezoelectric qualities following poling process treatment [1,2]. The four crystalline phases  $\alpha$ ,  $\beta$ ,  $\gamma$ , and  $\delta$  are observed based on the chain configuration of PVDF. resistance [3, 4–8]. The  $\delta$ -phase is ferroelectric and possesses a polar phase. The  $\alpha$  phase also has polar counterparts in the  $\beta$  and  $\gamma$ . Since they are affordable and have chemical resistance and biocompatibility, they are widely used in sensors, actuators, energy harvesting systems, batteries, filters, chemical warfare protection, magnetoelectric, and polymer-based composites [9-11]. In PVDF, the  $\beta$ -phase is distinguished by the highest spontaneous polarization and a certain chain shape per crystal unit cell. A number of processes have been thoroughly investigated in order to reveal the more electroactive  $\beta$ -phase in PVDF, involving phase transition, solvent casting, nucleating fillers, electrospinning, and copolymerization of PVDF [3, 12-15]. In the past decade, a lot of effort has been made to use the electrospinning technology to create fibers in the submicron range due to its higher quality and versatility [16,17]. Feeding the solution and applying a high voltage between the nozzle and collector stretches is necessary for the electrospinning setup, which turns the fluid into nanofibers. The conversion of the PVDF nanofibers from their mainly  $\alpha$ -phase to their  $\beta$ -phase can be influenced by a number of electrospinning process factors. The conversion of the PVDF nanofibers from their mainly  $\alpha$ -phase to their  $\beta$ -phase can be influenced by a number of electrospinning process factors [18]. In order to boost the  $\beta$ -phase in the produced PVDF nanofibers, a number of experiments have been conducted to optimize these characteristics. Several of the eight previously listed characteristics have been taken into account in the majority of these investigations [19]. The impact of various solvent

ratios, flow rate, spinning distance, and electrospinning voltage on the  $\beta$ -phase fraction was examined in a study by Gee et al. [20], the effect of DMF and acetone ratio, flow rate, spin distance and working temperature on the fraction of  $\beta$ -phase was studied. The impact of DMF and acetone ratio, flow rate, spin distance, and working temperature on the proportion of  $\beta$ -phase was examined in another parameter study conducted by Zheng et al. [21]. Yee et al. conducted a second investigation to examine the impact of DMF and acetone ratios on the  $\beta$ -phase fraction [22].

Applications for PVDF-based hydrophobic surfaces include anti-icing, sensing, pollution control, water treatment, oil-water separation, medicinal, and self-cleaning. Research into renewable resources, environmentally friendly solvents, and longer-lasting surface components is necessary for the sustainable production of PVDF nanocomposite materials. To handle trash from nanocomposite materials in an efficient and ecologically conscious way employing cutting-edge techniques like chemical and biological recycling, ongoing research is required.

In this work by using electrospinning equipment is gained highly aligned nano-magnetically enable PVDF-Fe<sub>3</sub>O<sub>4</sub> composite material for icephobic applications. Poling of PVDF was carried out to increase  $\beta$ -phase and an aligned molecular structure by using electric and magnetic field stretching at the same time as mechanical stretching forces.

### MATERIALS AND METHODS

#### Materials

Polyvinylidene fluoride (PVDF) pellet has  $M_w = 1.8 \times 10^4$  with linear chemical structure  $(-\text{CH}_2\text{CF}_2-)_n$  were pouched from Sigma-Aldrich, Fe<sub>3</sub>O<sub>4</sub> was obtained from Sigma-Aldrich with an average particle size of 20-30 nm. Acetone and N, N-dimethylformamide (DMF) were purchased from Sigma-Aldrich, Polysorbate Tween purchased from Sigma-Aldrich, Strong magnet, Metal bar

## Preparation of solutions

PVDF powders were dissolved in a mixture of organic solvents (DMF/acetone = 1/1 at 10 weight percent (w/w)) using a magnetic stirrer at a maximum temperature of 35°C for two hours at 35 rpm in a 250 ml beaker. Once the powders were fully dissolved, the Ultrasonic Cleaner Digital Pro was used for two hours to create a homogenous PVDF solution free of bubbles.

Initially, 50 milliliters of DMF were used to dissolve the Fe<sub>3</sub>O<sub>4</sub> nanoparticle powders, and 10 milliliters of Polysorbate Tween were added as a surfactant. The mixture was then stirred at 35 rpm for two hours at 30 degrees Celsius to create a solution with a 1 weight percent concentration. After that, sonication was done for two hours to obtain a non-homogenous solution. A two-phased solution was created following ultrasonication, and the electrospinning process used the top phase. Stretching the nanofibers using a mechanical force can organize the lamellae to create fibers aligned along the fiber axis and provide elongation forces during electrospinning [23].

In this study, mechanical stretching forces were achieved by simultaneously using electric and magnetic field stretching.

## Preparation PVDF/Fe<sub>3</sub>O<sub>4</sub> mats by electrospinning

The PVDF-Fe<sub>3</sub>O<sub>4</sub> composite material was made by increasing the speed of the rotating drum while only electrical field stretching was present. The parameters were 3000 rpm, 13 kV voltage, flow rates of 5 ml/hr for PVDF and 0.5 ml/hr for Fe<sub>3</sub>O<sub>4</sub>. The polymer and Fe<sub>3</sub>O<sub>4</sub> solution were fed into a dual channel programmable syringe pump, with each channel being independently controlled. The PVDF solution was electrospun at 13 kV voltage in a plastic syringe with a 20G needle. The PVDF solution flowed at 5 milliliters per hour. Five centimeters separated the collector and needle. A tubeless plastic syringe that was attached directly to the needle was used to inject the Fe<sub>3</sub>O<sub>4</sub> solution, saving money on costly nanoparticle material. The same syringe pump was used to inject Fe<sub>3</sub>O<sub>4</sub> solution into the syringe with a second 20G needle in order to create a magnetic field. 0.5 ml/h was the magnetite solution's flow rate. Figure 1 described the experimental setup. Using magnetic stretching to increase the alignment and crystallinity of PVDF could improve its wettability and icephobic properties. A strong magnetic field was attached to the electrospinning equipment's grinding line using a metal bar to create a magnetic field, and some magnetite (Fe<sub>3</sub>O<sub>4</sub>) molecules were drawn to the strong magnetic field. PVDF and Fe<sub>3</sub>O<sub>4</sub> solutions are injected onto the surface of the rotary drum. Since the Fe<sub>3</sub>O<sub>4</sub> molecules are attracted to the strong magnetic field, a small amount of the injected Fe<sub>3</sub>O<sub>4</sub> solution forms a thin thread between the magnetite syringe and the strong magnet, and the PVDF material is mechanically stretched by the magnetic field. PVDF and Fe<sub>3</sub>O<sub>4</sub> solutions are injected onto the surface of the rotary drum. Since the Fe<sub>3</sub>O<sub>4</sub> molecules are attracted to the strong magnetic field, a small amount of the injected Fe<sub>3</sub>O<sub>4</sub> solution forms an extremely thin thread

between the magnetite syringe and the strong magnet, and the PVDF material is mechanically stretched by the magnetic field.

## RESULTS AND DISCUSSION

### Microscopic and Morphological structure analysis

**Microscopic analysis.** Figure 2 displays microscopic analysis demonstrating the size and shape of the PVDF nanofibers. 10 kV was the acceleration voltage used in SEM imaging. The nanofibers made from 10% PVDF have a consistent shape devoid of twisting and beading patterns. Representative SEM micrographs of morphologically homogeneous surfaces taken at 1000–25,000 times magnification are displayed in Figure 2.

The PVDF/Fe<sub>3</sub>O<sub>4</sub> nanofiber material's highly aligned structure is seen in the SEM image with only a 10 μm scale bar (see fig. 2b)). These numbers show the development of ultrafine fibers with a diameter between 134 and 411 nm. Figure 3 shows that the fiber's average diameter is 224 nm. The fiber's average diameter is 224 nm. Electrospun nanofibers had a columnar shape and were consistent in morphology. Fe<sub>3</sub>O<sub>4</sub> nanoparticles are dispersed in twisting configurations on the PVDF/Fe<sub>3</sub>O<sub>4</sub> nanofiber coating, as demonstrated by the 10 μm picture, which was created by electrospinning with just a metal bar. A highly aligned sample was used to conduct additional research on PVDF/Fe<sub>3</sub>O<sub>4</sub> nanofiber coating for spectroscopic examination.

**X-Ray diffraction analysis (XRD).** The phases of different PVDF polymeric systems have been validated and identified using X-Ray diffraction analysis (XRD) data because XRD makes it easy to distinguish between the electroactive β phase and the nonelectroactive α phase. The produced samples were subjected to XRD examination using a Rigaku Mini Flex 600 XRD diffractometer. Using a Cu X-ray tube operated at 15 mA and 30 kV, CuK(α) radiation was employed for every case. The PVDF/Fe<sub>3</sub>O<sub>4</sub> nanocomposite was examined by X-ray diffraction investigation at room temperature, 25°C. Figure 4c) shows X-ray diffractogram of PVDF/Fe<sub>3</sub>O<sub>4</sub> nanocomposite with 10 wt% concentration. Figure 4a), Figure 4b) are the data preparation steps for Figure 4c). Red curve indicates PVDF, black curve indicates Fe<sub>3</sub>O<sub>4</sub> diffraction area. Red Curve (Lowest Intensity) shows a broad peak at lower angles, suggesting an amorphous or semi-crystalline phase. The intensity is relatively low, indicating a lower level of crystallinity. Black Curve (Highest Intensity) contains multiple sharp peaks, characteristic of a highly crystalline material. Blue Curve (Intermediate Intensity) displays a combination of broad and sharp peaks and indicates a mixture of crystalline and amorphous phases. Some sharp peaks suggest the presence of crystalline domains. Diffraction patterns were obtained in the range of Bragg's angle in a range: 5° - 100°. All diffraction peaks (2θ = 19°, 21°, 25°, 39°, 45°, 66°, 79°) are duly indexed from the JCPDC (Joint Committee on Powder Diffraction Standards). Strong diffraction peaks for 2θ = 21°, 39°, 45°, 66°, 79° assigned to β crystal phase of PVDF and lattice planes

of  $\text{Fe}_3\text{O}_4$  crystal with the cubic spinel structure. Weaker diffraction peaks for  $2\theta = 19^\circ, 25^\circ$  attributed to the 020, 021 reflections of the monoclinic  $\alpha$  crystal phase. The main X-ray peaks of  $\text{Fe}_3\text{O}_4$  solution were observed at  $39^\circ, 45^\circ, 66^\circ, 79^\circ$  which correspond to (311), (400), (440) and (444) are reflects to  $\text{Fe}_3\text{O}_4$  crystal with the inverse cubic spinel structure.

The discussion in this work concentrates on the crystalline phase, especially on the most common  $\alpha, \beta$  phases. As shown in XRD characterization figure 4c), the PVDF solution is mainly made of the  $\beta$  phase as evidenced by a strong peak at  $21^\circ$  corresponding to 110 reflection of the orthorhombic  $\beta$  phase. Presence of high intense peak at  $21^\circ$  confirms the presence of  $\beta$ -phase in PVDF film. Due to the medium electric voltage (13 kV) used during the electrospinning method, the random electric dipoles in the PVDF solution aligned, resulting in the forming of the  $\beta$  phase crystal structure. These results indicated that

electrospun nanofiber membranes contain mainly  $\beta$ -phase crystal structure of PVDF.

**CONCLUSIONS**

In this study, we synthesized PVDF/ $\text{Fe}_3\text{O}_4$  nanocomposite material, and the SEM pictures show that the aligned nanofibers were produced using the electrospinning technique. Using a directional electric field in electrospinning equipment, we obtained highly aligned nanofibrous film material to investigate their morphology structure. X-Ray diffraction analysis (XRD) was used to validate and identify the phases of PVDF polymeric systems, and the XRD analysis revealed that the PVDF solution is primarily composed of the  $\beta$  phase. These findings suggest that electrospun nanofiber membranes contain primarily the  $\beta$ -phase crystal structure of PVDF.

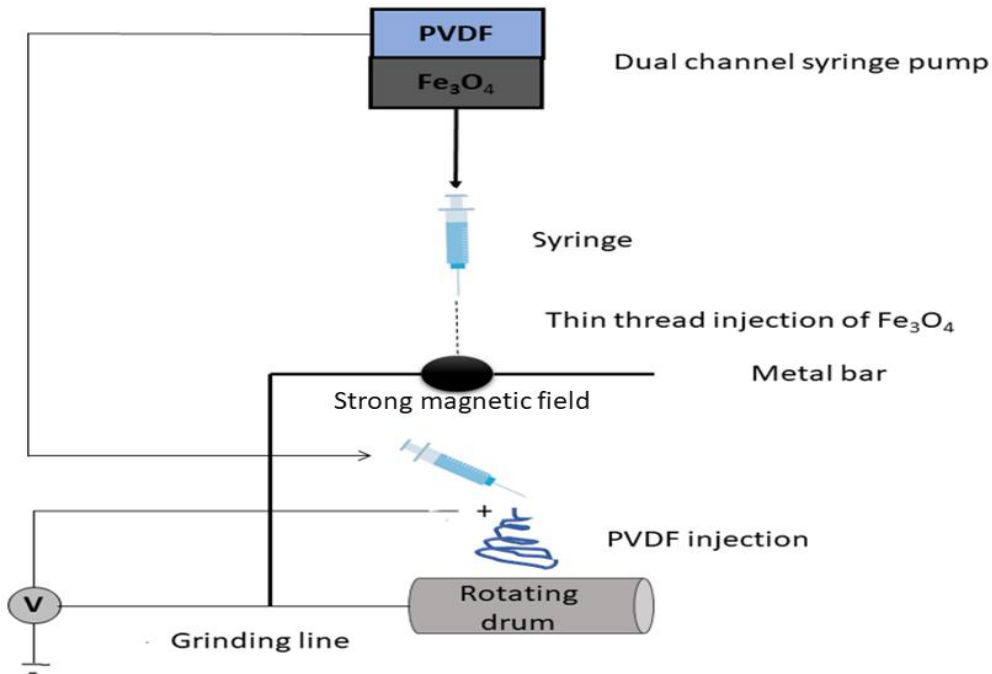


Fig. 1. Experimental set-up of electrospinning.

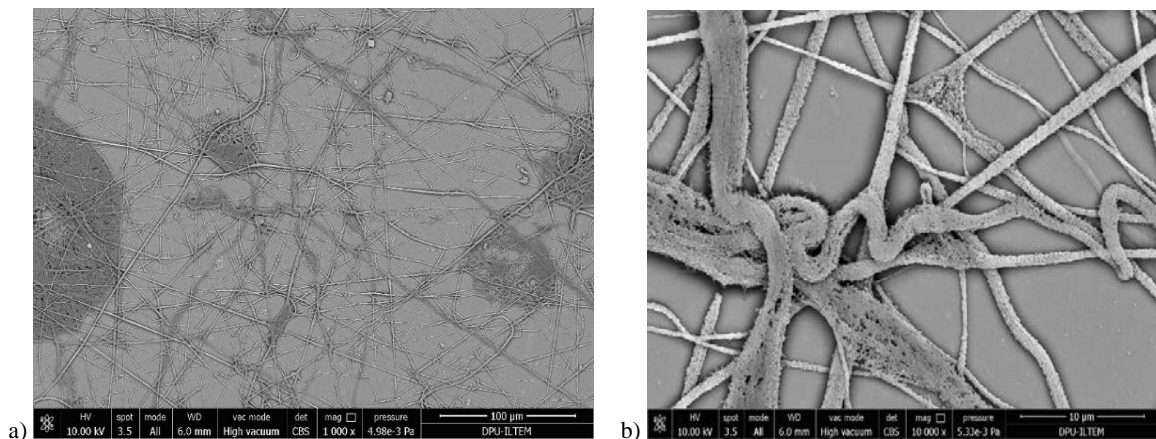
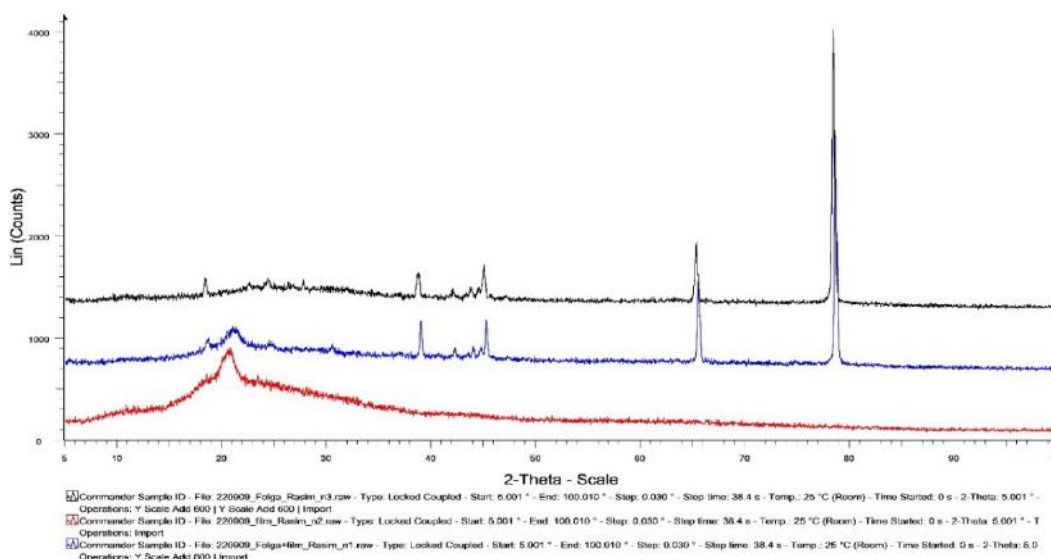


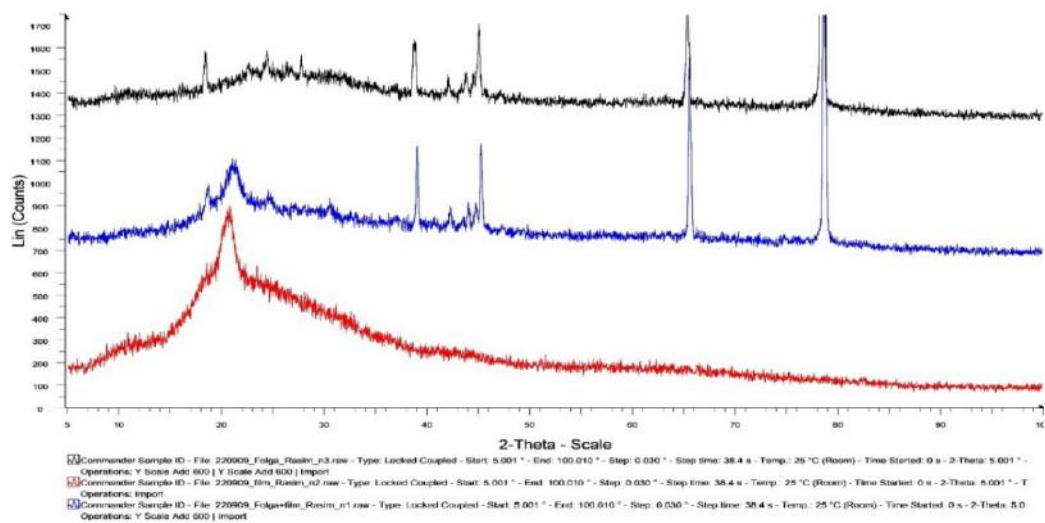
Fig. 2. SEM images of PVDF/ $\text{Fe}_3\text{O}_4$  nanofiber sample (Rotating Drum speed=3000 rpm; Voltage-13 kV) at a) 100  $\mu\text{m}$ , b) 10  $\mu\text{m}$  image.

	Label	Area	Mean	Min	Max	Angle	Length
1		0.005	154.259	65.167	190.984	-4.399	0.192
2		0.010	179.698	81.000	203.424	-53.746	0.411
3		0.003	196.690	110.000	219.333	-99.462	0.134
4		0.004	168.778	119.000	196.250	-172.875	0.178
5		0.005	188.078	147.000	203.333	-49.399	0.204
6		0.004	187.556	171.000	203.000	-90.000	0.177
7		0.007	186.102	125.000	206.408	-39.289	0.314
8		0.006	168.282	36.000	200.250	-131.634	0.266
9		0.005	219.182	155.000	246.000	-90.000	0.221
10		0.005	189.785	114.000	223.000	-36.870	0.221
11		0.005	189.219	124.000	208.667	-139.399	0.204
12		0.004	179.804	123.000	201.000	-105.945	0.161
13	Mean	0.005	183.953	114.181	208.471	-84.418	0.224
14	SD	0.002	16.216	38.042	14.778	49.264	0.076
15	Min	0.003	154.259	36.000	190.984	-172.875	0.134
16	Max	0.010	219.182	171.000	246.000	-4.399	0.411

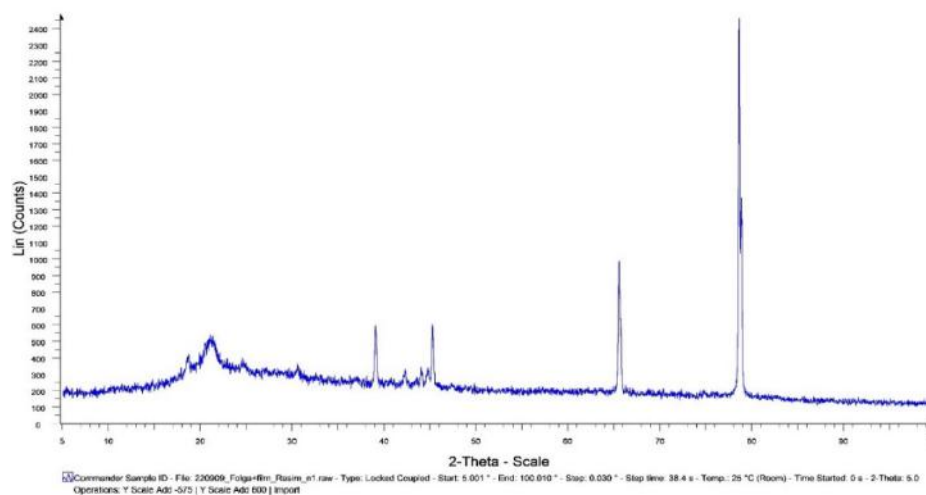
Fig. 3. Calculation average length size (diameter) of PVDF/Fe<sub>3</sub>O<sub>4</sub> nanofiber.



a)



b) X-ray diffraction pattern of PVDF/ Fe<sub>3</sub>O<sub>4</sub> nanofiber.



c)

Fig. 4. Data preparation steps of X-ray diffraction pattern of PVDF/Fe<sub>3</sub>O<sub>4</sub> nanofiber: 4a), 4b); X-ray diffraction pattern of PVDF/Fe<sub>3</sub>O<sub>4</sub> nanofiber: 4c).

- [1] S. Lanceros-Méndez, P. Martins. First Ed., Magnetolectric Polymer-Based Composites Fundamentals and Applications Wiley, Germany 2017.
- [2] P. Ueberschlag. Sens. Rev. 21, 118, 2001.
- [3] S. Bauer, F. Bauer. Springer Ser. Mater. Sci. 157 2008.
- [4] Z.W. Ouyang, E.C. Chen, T.M. Wu. Materials 8, 4553, 2015.
- [5] A.J. Lovinger. Science 220, 1115, 1983.
- [6] V. Sencadas, R.G. Filho, S. Lanceros-Mendez. J. Non-Cryst. Solids 352, 2226, 2006.
- [7] G. Botelho, S. Lanceros-Mendez, A.M. Goncalves, V. Sencadas, J.G. Rocha, J. N. G.T. Davis, J.E. McKinney, M.G. Broadhurst, S.C. Roth. J. Appl. Phys. 49, 4998, 1978.
- [8] N. Levi, R. Czerw, S. Xing, P. Iyer, D.L. Carroll. Nano Lett. 4, 1267, 2004.
- [9] J.Y. Lim, J. Kim, S. Kim, S. Kwak, Y. Lee, Y. Seo. Polymer 62, 11, 2015.
- [10] A.S. Motamedi, H. Mirzadeh, F. Hajiesmaeilb, J. Xu, M.J. Dapino, D. Gallego-Perez, D. Hansford. Sens. Actuators A 153, 24, 2009.
- [11] P. Martins, A.C. Lopes, S. Lanceros-Mendez. Prog. Polym. Sci. 39, 683, 2014.
- [12] S. Harstad, N. D'Souza, N. Soin, A.A. El-Gendy, S. Gupta, V.K. Pecharsky, T. Shah, E. Siores, R.L. Hadimani. AIP Adv. 7, 056411, 2017.
- [13] L. Ruan, X. Yao, Y. Chang, L. Zhou, G. Qin, X. Zhang. Polymers 10, 1, 2018.
- [14] Y.C. Ahn, S.K. Park, G.T. Kim, Y.J. Hwang, C.G. Lee, H.S. Shin, J.K. Lee. Curr. Appl. Phys. 6, 1030 2006.
- [15] C. Ribeiro, V. Sencadas, J.L.G. Ribelles, S. Lanceros-Méndez. Influence of processing conditions on polymorphism and nanofiber morphology of electroactive poly(vinylidene fluoride) electrospun membranes. Soft Mater. 8, 2010, 274–287.
- [16] S. Ramakrishna, K. Fujihara, W. Teo, T.-C. Lim, Z. Ma. An Introduction to Electrospinning and Nanofibers; World Scientific Publishing Company: Singapore, 2005
- [17] A. Haider, S. Haider, I.-K. Kang. A comprehensive review summarizing the effect of electrospinning parameters and potential applications of nanofibers in biomedical and biotechnology, Arab. J. Chem. 11 (2018) 1165–1188.
- [18] Rahul Kumar Singh, Sun Woh Lye, Jianmin Miao. Holistic investigation of the electrospinning parameters for high percentage of  $\beta$ -phase in PVDF nanofibers Polymer 214 (2021) 123366.
- [19] S. Gee, B. Johnson, A. Smith. Optimizing electrospinning parameters for piezoelectric PVDF nanofiber membranes, J. Membr. Sci. 563 (2018) 804–812.
- [20] J. Zheng, A. He, J. Li, C.C. Han. Polymorphism control of poly (vinylidene fluoride) through electrospinning, Macromol. Rapid Commun. 28 (2007) 2159–2162.
- [21] W.A. Yee, M. Kotaki, Y. Liu, X. Lu. Morphology, polymorphism behavior and molecular orientation of electrospun poly (vinylidene fluoride) fibers, Polymer 48 (2007) 512–521.
- [22] Zhou, Z.; Wu, X.-F. Electrospinning superhydrophobic-superoleophilic fibrous PVDF membranes for high-efficiency water-oil separation. Mater. Lett. 2015, 160, 423–427.

Received: 03.03.2025